ELSEVIER

https://www.jhltopen.org/

Computational pathology assessments of cardiac stromal remodeling: Clinical correlates and prognostic implications in heart transplantation

Eliot G. Peyster, MD, MSc,[a,*] Cai Yuan, PhD,[b] Sara Arabyarmohammadi, PhD,[b] Priti Lal, MD,[c] Michael D. Feldman, MD, PhD,[d] Pingfu Fu, PhD,[b] Kenneth B. Margulies, MD, MS,[a] and Anant Madabhushi, PhD, FAIMBE, FIEEE, FNAI[b,e,**]

[a]*Cardiovascular Research Institute, University of Pennsylvania, Philadelphia, Pennsylvania*
[b]*Department of Biomedical Engineering, Emory University and Georgia Institute of Technology, Atlanta, Georgia*
[c]*Department of Pathology and Laboratory Medicine, University of Pennsylvania, Philadelphia, Pennsylvania*
[d]*Department of Pathology & Laboratory Medicine, Indiana University School of Medicine, Indianapolis, Indiana*
[e]*Atlanta Veterans Administration Medical Center, Atlanta, Georgia*

KEYWORDS:
digital pathology;
cardiac remodeling;
cardiac stroma;
allograft rejection;
heart transplantation

BACKGROUND: The hostile immune environment created by allotransplantation can accelerate pathologic tissue remodeling. Both overt and indolent inflammatory insults propel this remodeling, but there is a paucity of tools for monitoring the speed and severity of remodeling over time.

METHODS: This retrospective cohort consisted of n = 2,167 digitized heart transplant biopsy slides along with records of prior inflammatory events and future allograft outcomes (cardiac death or allograft vasculopathy). Utilizing computational pathology analysis, biopsy images were analyzed to identify the pathologic stromal changes associated with future allograft loss or vasculopathy. Biopsy images were then analyzed to assess which historical inflammatory events drive progression of these pathologic stromal changes.

RESULTS: The top 5 features of pathologic stromal remodeling most associated with adverse allograft outcomes were also strongly associated with histories of both overt and indolent inflammatory events. Compared to controls, a history of high-grade or treated rejection was significantly associated with progressive pathologic remodeling and future adverse outcomes (32.9% vs 5.1%, $p < 0.001$). A history of recurrent low-grade rejection and Quilty lesions was also significantly associated with pathologic remodeling and adverse outcomes vs controls (12.7% vs 5.1%, $p = 0.047$). A history of high-grade or treated rejection in the absence of recurrent low-grade rejection history was not associated with pathologic remodeling or adverse outcomes (7.1% vs 5.1%, $p = 0.67$).

CONCLUSIONS: A history of both traditionally treated and traditionally ignored alloimmune responses can predispose patients to pathologic allograft remodeling and adverse outcomes. Computational pathology analysis of allograft stroma yields translationally relevant biomarkers, identifying accelerated remodeling before adverse outcomes occur.

*Corresponding author: Eliot G. Peyster, MD, MSc, Advanced Heart Failure and Transplant Medicine, Penn Cardiovascular Institute, University of Pennsylvania, Perelman Center for Advanced Medicine, 11 South Tower, Office 11-113, Philadelphia, PA 19104.

**Corresponding author: Anant Madabhushi, PhD, FAIMBE, FIEEE, FNAI, Wallace H. Coulter Department of Biomedical Engineering, Georgia Institute of Technology and Emory University, Health Sciences Research Building, 1750 Haygood Drive, Suite 647, Atlanta, GA 30322.

E-mail addresses: eliot.peyster@pennmedicine.upenn.edu, anantm@emory.edu.

https://doi.org/10.1016/j.jhlto.2024.100202

DATA AVAILABILITY: The data that support the findings of this study are presented in the manuscript and extended data sections. Unprocessed raw data are available from the corresponding author upon reasonable request. Source code for the stromal feature analysis pipeline is hosted on GitHub and freely available: https://github.service.emory.edu/CYUAN31/Pathomics_StromalBioMarker_in_Myocardium.git.
JHLT Open 2025;7:100202

Background

Immune-mediated damage of the transplanted heart is the primary cause of allograft failure and a primary focus of post-transplant medical care.[1-4] Established approaches for evaluating and characterizing the inflammatory processes affecting allograft health predominantly focus on the inflammatory cells themselves, rather than on the long-term effects of inflammation.[1-4] Endomyocardial biopsies (EMB) are routinely obtained, undergoing histologic grading based on the number, extent, and impact of infiltrating immune cells.[1,5] Newer "biopsy free" methods, such as peripheral blood gene expression profiling or cell-free DNA testing, are designed to reduce the burden of surveillance EMBs, but also focus on measurements of active immune cell activity/inflammatory damage to assess allograft health.[6-9]

While infiltrating immune cells are a primary cause of allograft injury, these cells themselves may not reflect the persistent allograft injury that has occurred. The morphologic correlates of the sustained allograft dysfunction which may result from inflammatory insults are mainly stromal processes affecting the extracellular matrix (ECM)[10-13] and are subtle and difficult to standardize with conventional histologic assessments. The cardiac stroma consists predominantly of fibroblasts, which undergo activation and differentiation under inflammatory conditions, leading to ECM remodeling via the deposition of thicker, more disordered collagen fibers.[14,15] Remodeling of the cardiac stroma perturbs normal myocardial structure, increasing stiffness, transducing maladaptive signals, and hindering substrate delivery and metabolic waste removal.[10-13,15-18] Indeed, it is long-term stromal remodeling driven by chronic and/or temporally remote immune-mediated damage that is thought to be the mechanism of "stiffening" observed in failing cardiac allografts and in those affected by cardiac allograft vasculopathy (CAV).[12,16,18-20]

There are no existing tools for measuring the microarchitectural changes that result from inflammatory processes in cardiac allografts. We assert that this represents an important limitation, both in documenting the effects of acute immune-mediated insults such as severe rejection events and in tracking the longer-term effects of more indolent, subclinical processes such as recurrent low-grade rejection or Quilty lesions. An assay capable of detecting the early, microscopic sequelae of pathologic remodeling could identify at-risk patients long before the development of overt, symptomatic, allograft dysfunction. This in turn could provide opportunities for early interventions, either in the form of intensified immunosuppression to quash indolent inflammation, therapeutics that have established roles in blunting pathologic remodeling in native hearts or emerging approaches that directly target stromal remodeling.[21]

In this study, we leverage computational pathology analysis to deeply interrogate the stromal microarchitecture of transplant EMB histology slides. Unlike recent studies utilizing computational pathology to assign International Society for Heart and Lung Transplantation (ISHLT) grades to EMB slides, the present study does not seek to reproduce work already performed by pathologists.[5,22] Instead, the focus is on developing a morphologic assay capable of extracting previously unavailable information from EMB histology samples via a rigorous, quantitative, first-in-field analysis of allograft stroma. Deploying this novel stromal assessment tool in more than 2,000 EMBs, we first establish the set of stromal "morphologic biomarkers" most strongly associated with long-term adverse allograft outcomes. We then evaluate how these novel morphologic biomarkers change over time following various alloimmune insults, assessing the impact on stromal remodeling of both overt allograft injury in the form of treated high-grade rejection, and the impact of untreated, indolent inflammation in the form of recurrent, low-grade rejection and Quilty lesions. By quantifying the specific impact on a tissue- and patient-level of these historical insults, we provide new insights into allograft biology and challenge conventional wisdom on which alloimmune processes merit therapeutic intervention.

Methods

Study cohort description, image quality control, and color normalization

The study cohort consisted of 2,167 hematoxylin and eosin (H&E)–stained EMB histology slides obtained from 650 patients treated between 1999 and 2016 at the Hospital of the University of Pennsylvania. Due to our interest in the impact of historical—rather than active—rejection events on allograft stroma, all study EMBs were confirmed to be free from serious rejection. Specifically, we excluded EMBs with any acute cellular rejections (ACR) ≥grade 2R, any antibody-mediated rejections (AMR) with a pathological AMR grade ≥grade 1,[1,4] and all treated rejections regardless of grade. Notably, only 6.6% of study EMBs (n = 162) underwent immunostaining for confirmatory AMR testing, as this has historically only been performed per provider request (rather

than per routine protocol) at the University of Pennsylvania. All slides underwent routine H&E assessments for AMR, utilizing criteria and definitions available at the time of clinical diagnosis. Histologic and clinical rejection diagnoses (cellular and antibody rejection grades, treated rejection history, and "Quilty" lesion presence) for all preceding EMB events were compiled for each study EMB, with totals for each diagnosis aggregated. Study EMBs were then assigned to the following "inflammatory history" subgroups: (1) all patients with a previous high-grade rejection (≥2R, ≥pAMR-1), or a treated rejection not otherwise specified), (2) the subset of subgroup 1 patients without recurrent low-grade or Quilty, (3) patients with recurrent low-grade rejection (≥3 grade 1R EMBs without any history of high-grade/treated rejection), (4) the subset of the subgroup 3 patients with recurrent low-grade and recurrent Quilty lesions (with ≥3 occurrences of each diagnosis), (5) frequent inflammatory events (any patient with >5 prior histologic diagnoses of Quilty, ACR ≥1R, and/or AMR ≥pAMR-1), and (6) controls, who met none of the other group inclusion criteria. Refer Figure 1 and Supplemental Methods for additional cohort details. Clinical data were collected for all patients contributing an EMB to the cohort, including selected, established, or purported donor and recipient risk factors for adverse allograft outcomes as listed in Table 1. Using these data, we identified patients with or without "adverse outcomes" defined as allograft loss (cardiovascular death or retransplantation) or ≥grade 2 CAV by 7-year post-transplant. A composite of cardiac death and ≥grade 2 CAV was chosen not only to enable adequate statistical power, but also because most cases of cardiac death in this cohort were out-of-hospital cardiac arrests. These "sudden death" events are frequently associated with progressive CAV, and although contemporary CAV testing was not performed for these cases, we consider it highly likely that they are etiologically similar enough to progressive CAV to be grouped together for our investigation. This research complies with the Declaration of Helsinki, and access to archival data and tissue was approved by the University of Pennsylvania Institutional Review Board, with waiver of consent authorized by 45. CFR.46.116(d) and 45. CFR.164.512(i).

All slides were digitized via whole-slide scanning at 40× magnification. Digitized slides underwent quality control assessments using HistoQC, an open-source, quantitative digital pathology analysis software tool for identifying artifacts and measuring slide quality.[23] A total of 265 slides were excluded from the study due to significant staining artifacts or damage to the archival slide. Color normalization was applied to each slide to account for slide and batch variations that can negatively impact image segmentation performance.[24]

Stromal fiber detection and feature analysis

Considering that different inflammatory processes act on different areas of cardiac stroma,[2,11,12,14,17,18] 3 distinct stromal subregions were considered for subsequent morphologic feature extraction: (1) endocardial stroma, (2) interstitial stroma, and (3) replacement stroma (Figure 2b). A total of 210 stromal features were extracted from each EMB slide. Broadly, these features pertain to 4 distinct categories, as outlined in Figure 2, and described in detail in Supplemental Methods. The first category describes the shape and size of stromal fibers: fiber length, fiber thickness (the total pixel size of the fiber divided by the fiber length), fiber solidity (the pixel ratio of a fiber and its smallest convex polygon), and fiber perimeter (obtained by the 8-direction chain code). The second feature category characterizes spatial orientation—the degree of local order/disorder—of stromal fibers, calculated locally within a 200-pixel neighborhood. The third category describes the accumulation and proliferation of stroma, including spatial density of the fibers (the number of stroma fibers in a certain pixel area) and the area ratio of cardiomyocytes to interstitial stroma. The fourth category describes the interaction between stromal fibers and cardiomyocytes, including assessing the angle and proximity of stromal fibers to the surrounding cardiomyocytes.

Data analysis and statistical methods

To identify morphologic biomarkers of stromal remodeling, we compared the time-dependent response of each extracted stromal feature between the composite Adverse Outcome group (allograft loss or CAV grade > 2 at 7 years) and the No Adverse Outcome group. Specifically, we constructed a mixed-effect regression model that includes variables for group, patient, time, and the interaction term between group and time.[25] In this model, the dependent variable was the examined stromal feature, and the independent variables were group, patient, and transplant time, with the interaction term formed by group and transplant time considered as a covariate to examine how stromal features respond to transplant time between different groups. By using this mixed-effects model to fit a regression line via the least-squares method, we were able to assess for significant differences in the change-over-time (from transplant) of stromal features between the Adverse Outcome group and the No Adverse Outcome group. The 5 features that exhibited the most significant differences in change-over-time (i.e., regression line slope) were selected and defined as the top features of "pathologic stromal remodeling." Using these features of pathologic stromal remodeling, we examined the inflammatory history subgroups, comparing stromal feature change-over-time in EMBs from patients in each subgroup vs controls. Last, inflammatory history subgroups were individually assessed for event rates using the composite Adverse Outcomes data. All statistical analysis was conducted in Python math package and Stata v.15.0 (StataCorp LLC). Figure 1 summarizes the experimental workflow from image analysis to data analysis.

Results

Cohort summary

Summary clinical data for the study cohort are shown in Table 1, with summary of outcomes experienced by subgroup shown in Table 2. As expected, there were numerous

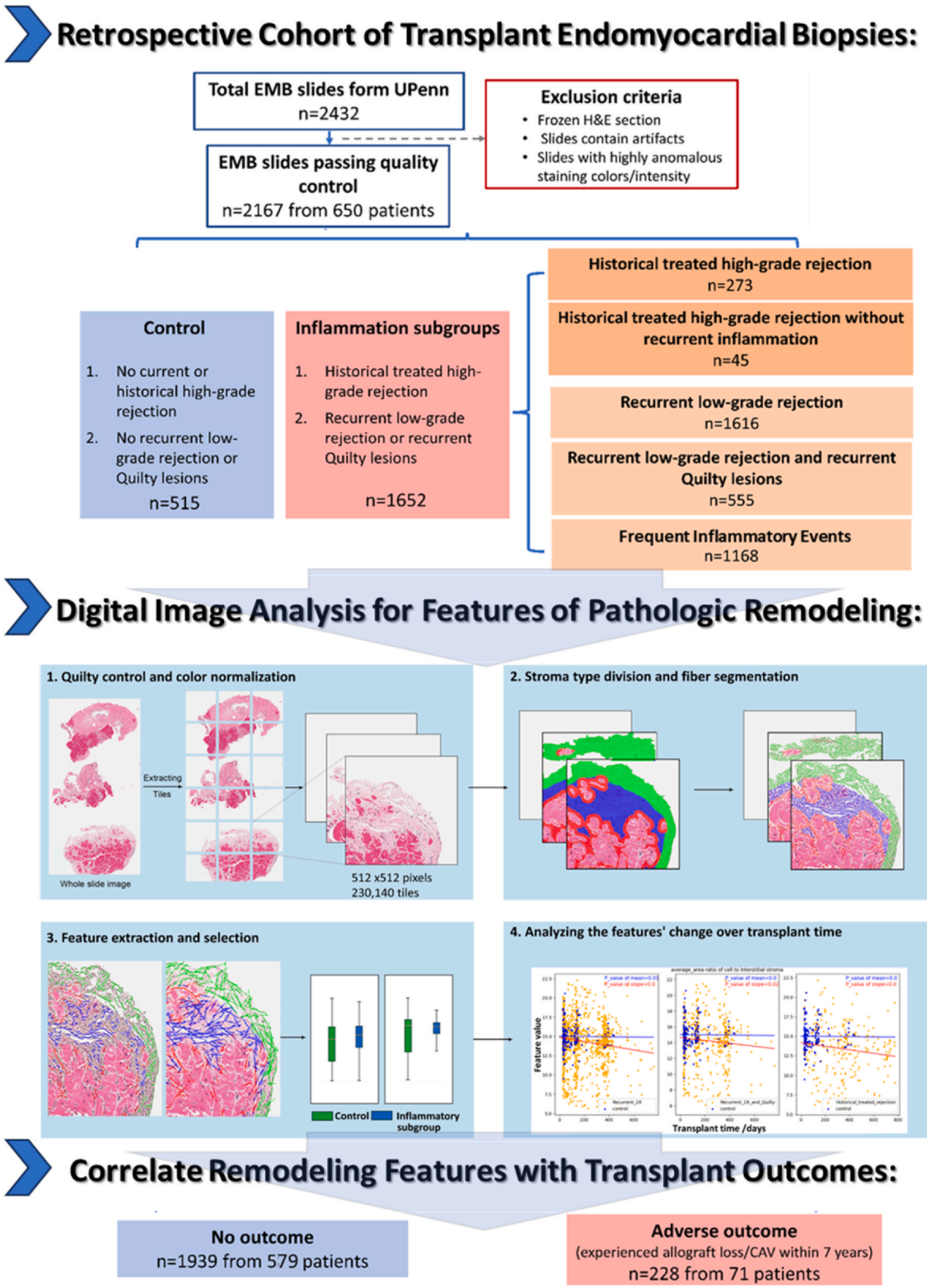

Figure 1 Study overview. At the top of the figure, a flowchart outlines the number of endomyocardial biopsy (EMB) slides in each inflammatory category. All EMBs can be categorized into 1 of 6 subgroups according to the historical events experienced by the patient before EMB acquisition, as shown in the figure. The middle section summarizes the computational pathology pipeline, including image quality control and color normalization, stromal morphologic feature segmentation and selection, and analysis of how each stromal feature changes over time between different inflammatory history subgroups. The length of the lines in middle section of panel 3, respectively, represents the size and orientation of stromal fibers. Different colors represent different types of stromal fibers in panels 2 and 3 (green: endocardial stroma, red: interstitial stroma, and blue: replacement stroma). The final section of the figure shows the number of patient- and EMB-level adverse outcomes experienced in the cohort, with adverse outcomes defined as the composite of allograft loss or CAV within 7 years. CAV, cardiac allograft vasculopathy; UPenn, University of Pennsylvania.

Table 1 Descriptive Statistics for Each of the Inflammatory Subgroups

Clinical variable	Full cohort (n = 650)	Controls (n = 98)	Recurrent low-grade rejection (n = 519)	Recurrent low grade and Quilty (n = 166)	Historical-treated or high-grade rejection (n = 85)	Historical-treated rejection without recurrent low grade/Quilty (n = 14)	> 5 Historical inflammatory events (n = 287)
Recipient race (%)							
• White	71%	64.3%	73% (p = 0.078)	71.7% (p = 0.209)	62.4% (p = 0.786)	42.9% (p = 0.123)	63.8% (p = 0.925)
• Black	17.9%	18.4%	18.5% (p = 0.975)	21.1% (p = 0.594)	22.4% (p = 0.503)	35.7% (p = 0.132)	26.5% (p = 0.106)
• Hispanic/Latin	2.1%	3.1%	1.9% (p = 0.473)	1.8% (p = 0.508)	3.5% (p = 0.859)	0% (p = 0.506)	3.8% (p = 0.724)
• Asian	1.4%	4.1%	0.8% (p = 0.007)	0.6% (p = 0.045)	1.2% (p = 0.229)	0% (p = 0.441)	0.7% (p = 0.019)
• Not specified	7.6%	10.1%	5.8% (p = 0.102)	4.8% (p = 0.093)	10.5% (p = 0.932)	21.4% (p = 0.220)	5.2% (p = 0.084)
Recipient sex (% male)	76.7%	77.6%	77.8% (p = 0.949)	80.7% (p = 0.537)	72.9% (p = 0.470)	64.3% (p = 0.277)	77.7% (p = 0.975)
Recipient age at transplant (mean in years)	52.3	53.9	52.2 (p = 0.248)	50.3 (p = 0.036)	48.1 (p = 0.002)	43.7 (p = 0.006)	51.7 (p = 0.143)
Retransplant	3.8%	2%	3.9% (p = 0.374)	4.8% (p = 0.253)	8% (p = 0.053)	7.1% (p = 0.268)	3.1% (p = 0.574)
BMI at 1-year post-transplant	28.2	30	28.1 (p = 0.029)	28.3 (p = 0.121)	28.6 (p = 0.166)	27.4 (p = 0.193)	29 (p = 0.273)
Recipient history of hypertension	32.9%	25.5%	33.5% (p = 0.119)	34.9% (p = 0.110)	50.6% ($p \leq 0.001$)	57.1% (p = 0.015)	45.6% ($p \leq 0.001$)
Recipient history of hyperlipidemia	34.9%	25.5%	35.4% (p = 0.056)	36.1% (p = 0.073)	41.2% (p = 0.024)	35.7% (p = 0.419)	41.1% (p = 0.005)
Recipient history of diabetes	37.7%	28.6%	38.7% (p = 0.056)	44.6% (p = 0.009)	36.4% (p = 0.254)	35.7% (p = 0.583)	40.4% (p = 0.036)
Recipient chronic kidney disease	54.9%	53.1%	56.1% (p = 0.582)	46.4% (p = 0.294)	52.9% (p = 0.987)	42.9% (p = 0.474)	60.2% (p = 0.210)
HLA mismatch (mean number)[a]	4.4	4.5	4.4 (p = 0.950)	4.6 (p = 0.306)	4.6 (p = 0.576)	4.6 (p = 0.575)	4.6 (p = 0.184)
CPRA score (% patients > 0)	4.8%	8.2%	4% (p = 0.077)	3% (p = 0.061)	3.5% (p = 0.188)	0% (p = 0.267)	2.8% (p = 0.021)
Positive donor–specific antibody[b]	7.1%	2%	7.5% (p = 0.046)	7.8% (p = 0.049)	16.5% ($p \leq 0.001$)	21.4% (p = 0.001)	14.3% ($p \leq 0.001$)
Donor age (mean in years)	37.2	37.3	37.1 (p = 0.787)	36.2 (p = 0.433)	39 (p = 0.478)	32.1 (p = 0.171)	37.4 (p = 0.926)
Donor hypertension	20.9%	21.4%	20.6% (p = 0.855)	16.3% (p = 0.293)	22.4% (p = 0.880)	21.4% (p = 1.0)	19.5% (p = 0.682)
Donor diabetes	6.8%	5.1%	9.4% (p = 0.163)	7.2% (p = 0.496)	9.4% (p = 0.257)	7.1% (p = 0.751)	7.7% (p = 0.390)

All *p-values are in comparison to Control* group.

Abbreviation: BMI, body mass index; CPRA, calculated panel reactive antibody; HLA, human leukocyte antigen.

[a]Defined based on number of mismatches in HLA-A, HLA-B, and HLA-DR, as per United Network for Organ Sharing database records.

[b]Defined as the percentage of patients who contributed a biopsy to the cohort after having a diagnosis of de-novo donor–specific antibody with mean fluorescent intensity > 1,500.

clinical risk factors associated with the adverse outcomes of allograft loss or CAV grade > 2 at 7 years, though Pearson correlation coefficients were generally modest (Supplemental Table S2). The correlation coefficients of 6 clinical risk factors with composite outcomes exceeded 0.1, revealing a weak correlation. These 6 risk factors are re-transplantation, body mass index at 1 year, diabetes, chronic kidney disease, donor age, and donor hypertension.

Prioritizing the morphologic biomarkers of stromal remodeling

The top 5 stromal morphologic features associated with the composite Adverse Outcomes are listed in Figure 3. Briefly, these stromal features describe the fiber density, solidity, and fiber orientation of the endocardial stroma, fiber thickness of interstitial stroma, and the area ratio of

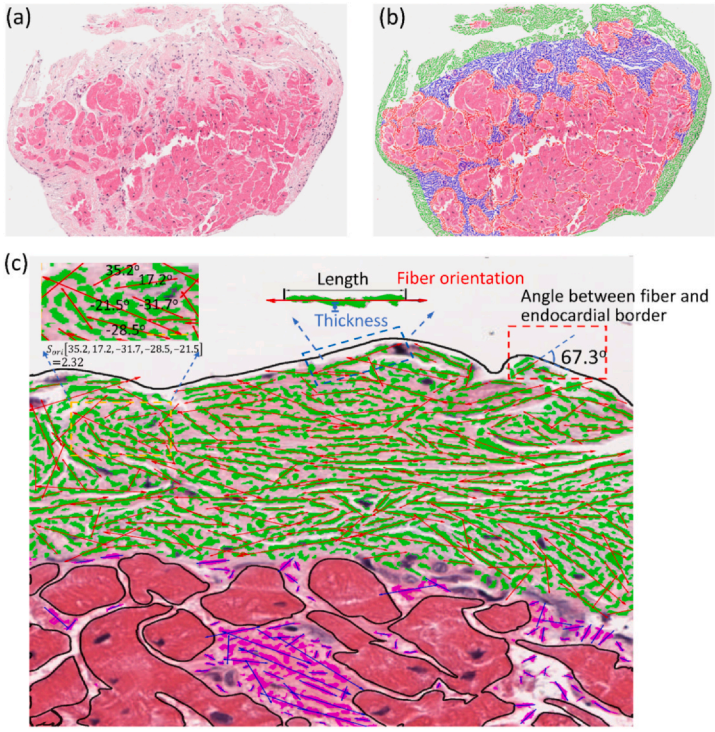

Feature family	Quantity	Feature description
Stromal fiber Shape	140	The length, thickness, curvature of the stromal fiber, etc.
Stromal fiber orientation entropy	30	Disorder of stromal fiber, etc.
Stroma accumulation	30	Fiber density metrics, both fiber number per area of stromal region, and as a ratio of stromal region
The interaction between stromal fiber and cardiomyocytes	10	Angle between stromal fiber and cardiomyocyte surface, etc.

Figure 2 Stromal feature identification workflow and annotated examples. The image on the left shows the workflow of feature extraction, including the division of stroma types, stromal fiber segmentation, and the extraction of stromal features. (a) Original H&E tissue staining image. (b) The effect of stroma type division (different colors represent different stroma types, green: endocardial stroma, red: interstitial stroma, blue: replacement stroma). (c) Representative examples of several extracted stromal features. The yellow box illustrates the local orientation entropy with the proximal 5 fibers. The blue box shows the length, thickness, and orientation of the fiber. The red box indicates the angle between the endocardial fiber and the endocardium boundary. The right table displays a summary of feature categories examined including fiber shape, orientation, stromal accumulation, and the interaction between fibers and myocytes. H&E, hematoxylin and eosin.

cardiomyocytes to interstitial stroma. These 5 features each exhibit statistically significant differences ($p < 0.05$ for all) in their trends over time-from-transplant between the No Outcome group and the Adverse Outcome group (Figure 3b). Figure 3c provides a more intuitive visualization of the differences in stromal features. Examination of non-interstitial stroma in the second and third columns shows that the endocardial stroma from the No Outcome group is more compact, with fibers that are shorter, less thick, less parallel, and with more delicate crosslinks. Examination of interstitial stroma in the fourth and fifth columns shows that the area, density, and length of interstitial stromal fibers are significantly increased in the Adverse Outcome group, suggesting proliferative interstitial remodeling.

Exploring the effects of previous inflammatory events on stromal remodeling

Plots of the change-over-time for each morphologic biomarker of pathologic remodeling in each historical inflammation subgroup vs controls are illustrated in Figure 4. There are numerous statistically significant differences in the slopes of the feature-change-over-time plots, suggesting that alloimmune events detected on prior biopsies induce measurable stromal changes which can be detected on subsequent biopsies. Notably, significant differences in pathologic remodeling were observed not only as a result of long-recognized risk factors such as a history of high-grade/treated rejection, but also in the indolent inflammation subgroups which have experienced recurrent 1R events and/or recurrent Quilty. Additionally, when EMBs that also have a history of recurrent, indolent inflammation (e.g., recurrent 1R or Quilty) are excluded, a history of high-grade/treated rejection alone no longer manifests significant differences in most pathologic stromal remodeling features compared to controls.

Examination of composite outcomes among patients contributing EMBs lends additional context to the in-situ stromal biomarker data. As seen in Table 2, patients contributing EMBs to several of the historical inflammation subgroups have significantly higher rates of adverse outcomes compared to patients contributing control biopsies (5.1% event rate). These include patients contributing historical high-grade/treated rejection biopsies (32.9%, $p < 0.001$), patients contributing recurrent low-grade and recurrent Quilty biopsies (12.7%, $p = 0.047$), and patients contributing recurrent inflammation biopsies (19.5%, $p < 0.001$). The recurrent low-grade alone group demonstrated an event rate nearly double control patients (9.4% vs 5.1%), though this was not significant ($p = 0.16$). Once again, a history of high-grade/treated rejection without a concurrent history of recurrent indolent inflammation did not confer increased risk (7.1%, $p = 0.67$). Taken together, the EMB

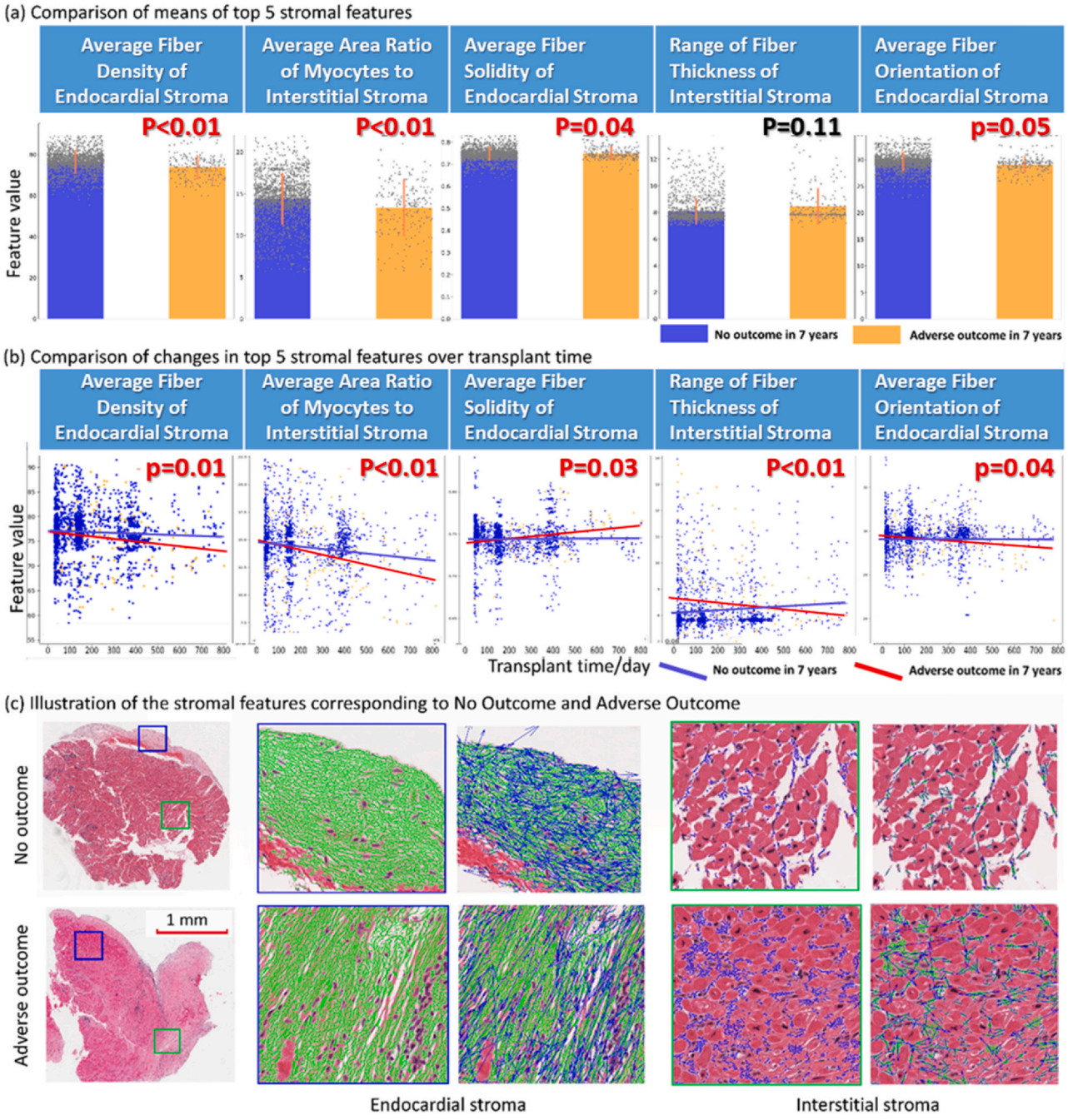

Figure 3 Prioritized stromal biomarkers of remodeling, identified based on significant changes over time from transplant between the Composite Adverse Outcome group and the No Outcome group. (a) Comparison of the mean values of the top 5 stromal features between the Composite Adverse Outcome group and the No Outcome group. (b) Changes in the top 5 stromal features over transplant time. The blue lines indicate linear fit from the No Outcome group, and orange lines indicate the linear fit from the Composite Adverse Outcome group. Note that in the fourth panel, there is an obvious and significant difference in the slopes for the 2 linear fits—a result that is obscured in the fourth panel of this figures section (a) which utilized average feature values instead of change-over-time values. (c) Illustrative examples of tissue from a patient in the Composite Adverse Outcome group and the No Outcome group. The first column corresponds to the original H&E image, in which the colored squares indicate the sampling sites: blue corresponds to endocardial stroma, and green corresponds to interstitial stroma. The second and fourth columns show the identified endocardial and interstitial stromal tissue after segmentation, respectively. The third and fifth columns show the discrete endocardial and interstitial fibers, with each fiber assigned a vector arrows. The number, length, and orientation of vectors indicate the density, length, and orientation of the segmented stromal fiber.

and patient subgroup analyses suggest that inflammatory insults such as recurrent Quilty lesions and low-level rejection—which are typically not treated in clinical practice—induce measurable changes to the allograft stroma and may be associated with poor patient outcomes.

Discussion

In this article, we describe the development of a computational pathology analysis pipeline designed to comprehensively characterize the stromal architecture of cardiac

Table 2 Adverse Outcome[a] Event Rate for Patients Contributing Biopsies to Each Historical Inflammation Subgroup

Group	Number of patients contributing biopsies	Number of events	Event rate (*p*-value vs control)
Control	98	5	5.1% (NA)
Recurrent low-grade rejection	519	49	9.4% (0.16)
Recurrent low-grade and Quilty	166	21	12.7% (0.047)
Historical-treated or high-grade rejection	85	28	32.9% (< 0.001)
Historical-treated/high-grade rejection without recurrent low-grade/Quilty	14	1	7.1% (0.67)
> 5 Historical inflammatory events	287	56	19.5% (< 0.001)

Abbreviation: CAV, cardiac allograft vasculopathy.
[a]Adverse outcomes defined as allograft loss or > grade 2 CAV by 7-year post-transplant.

allografts. Evaluating this pipeline on a large cohort of heart transplant EMBs, we examined the effects of allo-immunity from a novel perspective; focusing on the chronic stromal changes induced by inflammatory insults rather than on the inflammatory cells that induce those changes. Traditional histologic assessments of transplant EMBs such as ISHLT rejection grading focus predominantly on infiltrating inflammatory cells and their immediate effects.[1] Recent computational pathology research in transplant medicine has focused predominantly on reproducing these traditional histologic assessments,[5,22] and as a result, are largely constrained to the same, well-documented, limitations as the ISHLT grading framework. Our approach highlights the value of moving beyond this conventional framework, leveraging digital image analysis to monitor subtle morphologic changes occurring in EMBs over time, then identifying the core set of morphologic changes that portend poor long-term patient outcomes. We assert that future applications of digital pathology would benefit from adopting a similar approach, utilizing longitudinal samples and statistics to correlate progressive morphologic changes with hard clinical end-points.

From a histopathology perspective, the morphologic features of pathologic remodeling we identified provide a detailed view of how the cardiac stroma is changed by different inflammatory insults. Historical inflammatory insults resulted in an increase in interstitial stroma area relative to myocyte area, a finding consistent with the myocyte loss and interstitial fibrosis that can result from immune-mediated myocardial injury.[5,11,15,18,20] In addition, relative to controls, historical inflammatory insults increased stromal fiber thickness, solidity, and parallelism (e.g., less disordered/branched fibers). This may be explained by the progressive deposition of type I collagen after an inflammatory injury. Type I and type III collagen are the main structural constituents of the cardiac ECM, with type I collagen manifesting thicker, straighter, and more parallel fibers while type III collagen manifests finer, wavier, and more intricately branched fibers.[10,17,18] It has been shown that rejection and other inflammatory insults can cause the proportion of type I collagen to increase relative to the type III collagen,[11,15,17,18] resulting in a "stiffer" myocardium. This may explain both the aforementioned stromal features which differentiated EMBs with more/more severe historical inflammatory events from controls, and may explain the poorer long-term outcomes associated with these features. Last, although stroma area was increased, the apparent number/density of fibers in the stroma was reduced in EMBs with historical inflammation. Whether this results from different collagen subtypes, from nonfibrous ECM proliferation, from edema due to indolent inflammation, or from increased stroma "cellularity" (which contributes to stroma area while increasing the space between individual fibers), cannot be definitively answered from this study. However, each is a potential mechanism worthy of exploration in future research.

The experiments reported in this article yielded several findings of translational value. First, identifying the progressive stromal changes that are most strongly correlated with future adverse outcomes creates opportunities for intervention, either through augmented immunosuppression, through the use of traditional heart failure therapeutics with "reverse remodeling" capability, or by application of new treatments that directly target stromal remodeling.[21] Whether the specific biomarkers of pathologic remodeling uncovered in this experiment can be used to monitor treatment effects after a therapeutic intervention remains unknown, but is an additional potential application for the novel stromal biomarkers reported in this paper. Moreover, the finding that recurrent low-grade inflammatory processes are linked to adverse long-term outcomes is significant and worthy of further discussion.

It is common practice for transplant clinicians to monitor, but not treat, low-grade ACR events and Quilty lesions, only implementing acute or chronic therapeutic interventions for cases involving clinical evidence of allograft dysfunction. In fact, current ISHLT guidelines generally discourage treatment of low-grade ACR events.[26] On the other hand, most episodes of "high-grade" rejection as defined in this article (either ACR ≥2R or pAMR > 0) undergo either acute treatment or alterations of chronic immunosuppression, largely in accordance with existing guidelines.[26,27] In the present study, our results show that recurrent, indolent inflammatory processes such as low-grade ACR and Quilty lesions are associated with significant, pathologic changes in the cardiac stroma, and that this leads to a higher incidence of adverse allograft outcomes. In addition, our results showed that isolated

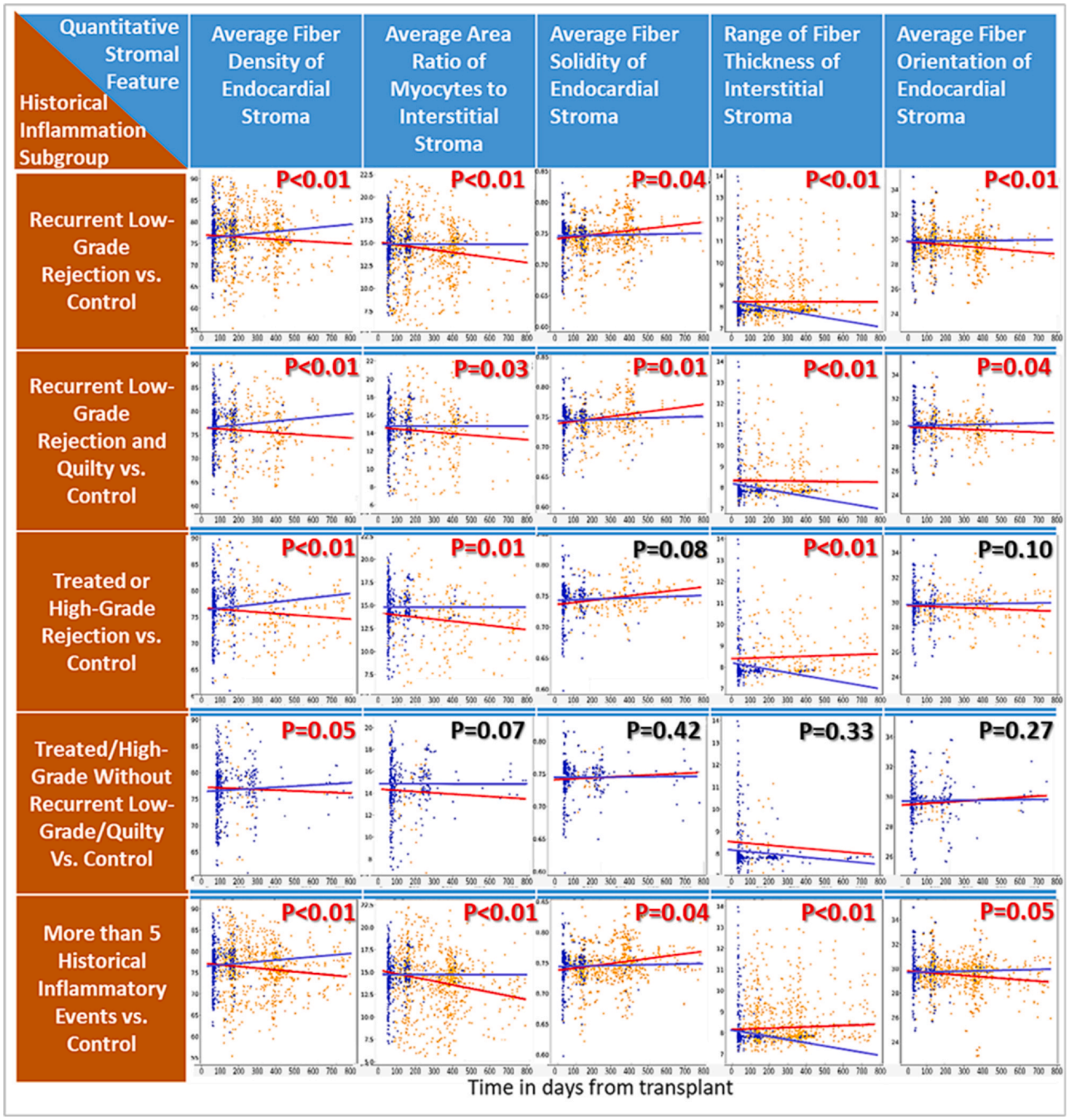

Figure 4 Time-dependent trajectories of prioritized morphologic biomarkers. Each row represents comparison to controls of 1 of the 5 patient subgroups based on a history of rejection diagnoses. Each column represents 1 of the morphologic biomarkers of pathologic rejection, selected based on strength of association with adverse patient outcomes. Blue linear fit lines represent the Control group (which is derived from the individual blue data points), while the red linear fit lines represent the Inflammatory group (which is derived from the individual yellow data points). *p*-values generated via mixed-effects modeling in each panel are derived from comparisons of linear fit slopes for Controls and Inflammatory groups.

episodes of high-grade rejection in patients without a history of recurrent 1R or Quilty do not appear to induce significant long-term pathologic changes in the cardiac stroma. In the context of current practice patterns and guidelines, these findings suggest that clinicians may be undervaluing the importance of chronic "mild" alloimmune responses, and may be—in some cases—overvaluing the impact of isolated, high-grade histologic rejection.

Prior research has shown correlations between Quilty lesions and adverse outcomes, though the available literature has conflicting findings.[1,2,20,28] The impact of recurrent low-grade ACR on transplant outcomes has not been studied as frequently, though recent research does suggest that a history of higher "average" rejection grades (even in the absence of high-grade events) is associated with a higher incidence of early CAV.[20] While in this article our findings generally support a connection between recurrent, untreated, indolent inflammation and adverse events, it is clear that not all patients with a history of Quilty and/or low-grade ACR necessarily suffer poor

outcomes. Moreover, due to the retrospective nature of this research, there is no way to assess the potential risks or benefits that might arise from altering immunosuppression based on a history of recurrent indolent inflammation alone. Nevertheless, given the strong correlation between pathologic remodeling features and poor outcomes in these patients, it is worth considering a potential clinical role for our stromal biomarkers. EMB samples are already obtained as part of routine care, and digital pathology analysis pipelines can be quickly and remotely accessed through cloud-based systems. Thus, while future clinical investigations are clearly needed, protocols that incorporate predictive morphologic biomarkers into immunosuppression management and CAV screening decisions might prove to be feasible and valuable.

As the field gradually pivots toward rejection surveillance paradigms that utilize more peripheral blood-based assays (e.g., cell-free DNA, gene expression profiling) and fewer EMBs,[6-9] we assert that it will become increasingly important to rely on digital pathology biomarkers such as those in this article. If patients are to receive only 3 to 4 EMBs during their post-transplant course, then it is critical to extract maximum information from each of these events. The fewer EMBs performed, the lower the likelihood of identifying patients who are experiencing poor-outcome–associated recurrent 1R and Quilty lesions. Thus, it will be necessary to rely on surrogates for these recurrent histologic diagnoses, such as the biomarkers of pathologic stromal remodeling which we identified in this article and which have clear associations with adverse outcomes. Future rejection surveillance protocols could therefore rely primarily on serologic testing, with EMBs performed at a few, widely spaced intervals to enable monitoring of subtle, serial changes that help identify at-risk populations. Compared to traditional, biopsy-heavy approaches relying on conventional histologic grading, such a hybrid approach, could maximize personalization while still minimizing invasive testing. Correlating the deep, quantitative, microarchitectural changes described in this article with macroarchitectural findings from cardiac magnetic resonance imaging represents another potential future direction that could both reduce invasive testing burden while maximizing the prognostic value of allograft testing.

As with all research, this study has limitations. Although the cohort comprised over 2,000 biopsies, this was a single-center study, and there were relatively few patients in the interesting "previous high-grade rejection without recurrent low-grade or Quilty" subgroup. Additionally, while we utilized all available histologic diagnoses associated with study EMBs, additional, unmeasured, alloimmune processes could have confounded our findings. Due to the limited application of immunostaining at our center on routine screening EMBs, our historical cohort precluded a complete and definitive assessment of AMR in many cases. While we can confidently evaluate whether histologic criteria for AMR are met (i.e., pAMR(h+)), our ability to determine whether immunologic markers are present (i.e., pAMR-(i+)) was limited to those EMBs that underwent immunostaining. Another unavoidable limitation of this study is the reliance on pathology diagnostic records for assigning "inflammatory history" case labels. It is well known that there is significant interpathologist variability in the application of ISHLT grades to transplant EMBs.[5,29,30] Thus, study labels such as "previous high-grade rejection" or "recurrent low-grade rejection" (without a history of high-grade rejection) are not definitively accurate. The fact that different pathologists would likely grade historical EMBs differently means that there is inevitable overlap between some study subgroups. It should be noted that while this limitation may affect subgroup comparisons, it has no impact on the correlations between specific patterns of stromal remodeling and patient-level clinical outcomes—a fact that further highlights the need for grounding computational pathology research in definitive clinical endpoints rather than imperfect histologic reference standards.

In conclusion, this study represents a novel and important application of computational pathology analysis within heart transplant medicine. Focusing on the allograft tissue itself rather than on the infiltrating immune cells, the stromal morphologic biomarkers described in this article demonstrate the ability to quantify the effects of various historical inflammatory insults, uncovering new information about how different histories may predispose patients to adverse clinical outcomes.

Author contributions

Eliot Peyster: study design, data collection, data analysis, manuscript writing, and acquisition of funding. Cai Yuan: study design, data analysis, and manuscript writing. Anant Madabhushi: study design, data analysis, manuscript writing, and acquisition of funding. Kenneth Margulies: study design, manuscript writing, acquisition of funding. PingFu Fu: data analysis, manuscript writing. Priti Lal: manuscript writing, study design. Michael Feldman: manuscript writing, study design.

Disclosure statement

Dr Feldman is an equity holder and has technology licensed to both Elucid Bioimaging and Inspirata Inc. Dr Feldman is a scientific advisory consultant for Inspirata Inc and sits on its scientific advisory board. Dr Feldman is also a consultant for Phillips Healthcare, XFIN, and Virbio. Dr Margulies holds research grants from Amgen and serves as a scientific consultant/advisory board member for Bristol Myers Squibb. Dr Madabhushi is an equity holder in Elucid Bioimaging, Inspirata Inc, and Picture Health. In addition, he has served as a scientific advisory board member for Picture Health, SimbioSys, and Aiforia Inc. He also has sponsored research agreements with Astrazeneca, Bristol Myers Squibb, Boehringer-Ingelheim, and Eli-Lilly. His technology has been licensed to Elucid Bioimaging and Picture Health. He is also involved in 3 different NIH R01 grants with Inspirata Inc.

Research reported in this publication was supported by the National Cancer Institute under award numbers R01CA268287A1, U01CA269181, R01CA26820701A1, R01CA249992-01A1, R01CA202752-01A1, R01CA208236-01A1, R01CA216579-01A1, R01CA220581-01A1, R01CA257612-01A1, 1U01CA239055-01, 1U01CA248226-01, 1U54CA254566-01; National Heart, Lung and Blood Institute 1R01HL15127701A1, R01HL15807101A1; K08HL159344, National Institute of Biomedical Imaging and Bioengineering 1R43EB028736-01; VA Merit Review Award IBX004121A from the United States Department of Veterans Affairs Biomedical Laboratory Research and Development Service the Office of the Assistant Secretary of Defense for Health Affairs, through the Breast Cancer Research Program (W81XWH-19-1-0668), the Prostate Cancer Research Program (W81XWH-20-1-0851), the Lung Cancer Research Program (W81XWH-18-1-0440, W81XWH-20-1-0595), the Peer Reviewed Cancer Research Program (W81XWH-18-1-0404, W81XWH-21-1-0345, W81XWH-21-1-0160), the Kidney Precision Medicine Project (KPMP) Glue Grant, the W.W. Smith Charitable Trust, the Bogle Family Foundation, and sponsored research agreements from Bristol Myers Squibb, Boehringer-Ingelheim, Eli-Lilly and AstraZeneca.

Appendix A. Supplementary data

Supplementary data associated with this article can be found in the online version at doi:10.1016/j.jhlto.2024.100202.

References

1. Stewart S, Winters GL, Fishbein MC, et al. Revision of the 1990 working formulation for the standardization of nomenclature in the diagnosis of heart rejection. J Heart Lung Transplant 2005;24:1710-20.
2. Duong Van Huyen JP, Fedrigo M, Fishbein GA, et al. The XVth Banff conference on allograft pathology the Banff workshop heart report: improving the diagnostic yield from endomyocardial biopsies and quilty effect revisited. Am J Transplant 2020;20(12):3308-18.
3. Khush KK, Cherikh WS, Chambers DC, et al. The International Thoracic Organ Transplant Registry of the International Society for Heart and Lung Transplantation: thirty-sixth adult heart transplantation report - 2019; focus theme: donor and recipient size match. J Heart Lung Transplant 2019;38:1056-66.
4. Berry GJ, Burke MM, Andersen C, et al. The 2013 International Society for Heart and Lung Transplantation Working Formulation for the standardization of nomenclature in the pathologic diagnosis of antibody-mediated rejection in heart transplantation. J Heart Lung Transplant 2013;32:1147-62.
5. Peyster EG, Arabyarmohammadi S, Janowczyk A, et al. An automated computational image analysis pipeline for histological grading of cardiac allograft rejection. Eur Heart J 2021;42:2356-69.
6. Khush KK, Patel J, Pinney S, et al. Non-invasive detection of graft injury after heart transplantation using donor-derived cell-free DNA: a prospective multi-center study. Am J Transplant 2019;19(10):2889-99.
7. Mavrogeni SI, Athanasopoulos G, Gouziouta A, Leontiadis E, Adamopoulos S, Kolovou G. Cardiac transplantation: towards a new noninvasive approach of cardiac allograft rejection. Expert Rev Cardiovasc Ther 2017;15:307-13.
8. Crespo-Leiro MG, Stypmann J, Schulz U, et al. Clinical usefulness of gene-expression profile to rule out acute rejection after heart transplantation: CARGO II. Eur Heart J 2016;37:2591-601.
9. De Vlaminck I, Valantine HA, Snyder TM, et al. Circulating cell-free DNA enables noninvasive diagnosis of heart transplant rejection. Sci Transl Med 2014;6(241):241ra77.
10. Franz M, Neri D, Berndt A. Chronic cardiac allograft rejection: critical role of ED-A(+) fibronectin and implications for targeted therapy strategies. J Pathol 2012;226:557-61.
11. Tazelaar HD, Gay RE, Rowan RA, Billingham ME, Gay S. Collagen profile in the transplanted heart. Hum Pathol 1990;21:424-8.
12. Jansen MAA, Otten HG, de Weger RA, Huibers MMH. Immunological and fibrotic mechanisms in cardiac allograft vasculopathy. Transplantation 2015;99(12):2467-75.
13. Hiemann NE, Wellnhofer E, Lehmkuhl HB, Knosalla C, Hetzer R, Meyer R. Everolimus prevents endomyocardial remodeling after heart transplantation. Transplantation 2011;92(10):1165-72.
14. Díez J, González A, Kovacic JC. Myocardial interstitial fibrosis in nonischemic heart disease, part 3/4: JACC focus seminar. J Am Coll Cardiol 2020;75:2204-18.
15. Frangogiannis NG, Kovacic JC. Extracellular matrix in ischemic heart disease, part 4/4: JACC focus seminar. J Am Coll Cardiol 2020;75:2219-35.
16. Vejpongsa P, Torre-Amione G, Marcos-Abdala HG, et al. Long term development of diastolic dysfunction and heart failure with preserved left ventricular ejection fraction in heart transplant recipients. Sci Rep 2022;12:3834.
17. Weber KT. Cardiac interstitium in health and disease: the fibrillar collagen network. J Am Coll Cardiol 1989;13:1637-52.
18. Frangogiannis NG. The extracellular matrix in ischemic and nonischemic heart failure. Circ Res 2019;125:117-46.
19. Chih S, Chong AY, Mielniczuk LM, Bhatt DL, Beanlands RSB. Allograft vasculopathy: the Achilles' heel of heart transplantation. J Am Coll Cardiol 2016;68:80-91.
20. Peyster EG, Janowczyk A, Swamidoss A, Kethireddy S, Feldman MD, Margulies KB. Computational analysis of routine biopsies improves diagnosis and prediction of cardiac allograft vasculopathy. Circulation 2022;145:1563-77.
21. Morfino P, Aimo A, Castiglione V, Gálvez-Montón C, Emdin M, Bayes-Genis A. Treatment of cardiac fibrosis: from neuro-hormonal inhibitors to CAR-T cell therapy. Heart Fail Rev 2023;28:555-69.
22. Lipkova J, Chen TY, Lu MY, et al. Deep learning-enabled assessment of cardiac allograft rejection from endomyocardial biopsies. Nat Med 2022;28:575-82.
23. Janowczyk A, Zuo R, Gilmore H, Feldman M, Madabhushi A. HistoQC: an open-source quality control tool for digital pathology slides. JCO Clin Cancer Inform 2019;3:1-7.
24. Reinhard E, Adhikhmin M, Gooch B, Shirley P. Color transfer between images. IEEE Comput Graph Appl 2001;21:34-41.
25. Laird NM, Ware JH. Random-effects models for longitudinal data. Biometrics 1982;38:963-74.
26. Velleca A, Shullo MA, Dhital K, et al. The International Society for Heart and Lung Transplantation (ISHLT) guidelines for the care of heart transplant recipients. J Heart Lung Transplant 2023;42:e1-141.
27. Chih S, Tinckam KJ, Ross HJ. A survey of current practice for antibody-mediated rejection in heart transplantation. Am J Transplant 2013;13:1069-74.
28. Cho H, Choi JO, Jeon ES, Kim JS. Quilty lesions in the endomyocardial biopsies after heart transplantation. J Pathol Transl Med 2019;53:50-6.
29. Crespo-Leiro MG, Zuckermann A, Bara C, et al. Concordance among pathologists in the second Cardiac Allograft Rejection Gene Expression Observational Study (CARGO II). Transplantation 2012;94:1172-7.
30. Peyster EG, Madabhushi A, Margulies KB. Advanced morphologic analysis for diagnosing allograft rejection: the case of cardiac transplant rejection. Transplantation 2018;102:1230-9.